Received: 7 August 2020 | Accepted: 25 January 2021

DOI: 10.1002/csc2.20473

Crop Science

ORIGINAL RESEARCH ARTICLE

Plant Genetic Resources

Coexpression gene network analysis of cold-tolerant *Solanum commersonii* reveals new insights in response to low temperatures

Salvatore Esposito[1,†] | **Riccardo Aversano**[2,†] | **James Bradeen**[3] | **Vincenzo D'Amelia**[4] | **Clizia Villano**[2] | **Domenico Carputo**[2]

[1] CREA Research Centre for Cereal and Industrial Crops (CREA-CI), S.S. 673, km 25.200, Foggia 71122, Italy

[2] Department of Agricultural Sciences, University of Naples Federico II, Portici 80055, Italy

[3] Department of Plant Pathology and The Stakman-Borlaug Center for Sustainable Plant Health, University of Minnesota, St. Paul, MN, USA

[4] Institute of Biosciences and Bioresources, Research Division Portici, Consiglio Nazionale delle Ricerche, Portici 80055, Italy

Correspondence
Domenico Carputo, Department of Agricultural Sciences, University of Naples Federico II, Portici, 80055 Italy.
Email: carputo@unina.it

[†]These authors contributed equally to the manuscript

Assigned to Associate Editor Randy Dinkins.

Funding information
University of Naples Federico II

Abstract

Among abiotic stressors, cold is one of the most harmful for the cultivated potato (*Solanum tuberosum* L.), a frost-sensitive crop. RNA sequencing (RNA-seq) profiling of two different clones of wild potato (*S. commersonii* Dun.) contrasting in their capacity to withstand low temperatures revealed a higher number of differentially expressed genes (DEGs) under nonacclimated conditions (NAC) in tolerant clone cmm1T vs. the susceptible cmm6-6 (1,002 and 8,055 DEGs, respectively). By contrast, the number of DEGs was much more comparable when both genotypes were under acclimated conditions (AC). Indeed, a total of 5,650 and 8,936 DEGs were detected in the tolerant genotype vs. the susceptible. Gene ontology (GO) classification under NAC showed a significant role for transcription regulation, lignin catabolic genes, and regulation of plant type secondary cell wall in the cold-tolerant genotypes, suggesting an important role in conferring tolerance response. By contrast, response to stress and response to stimuli were enriched GO categories in both clones under AC. Unsigned weighted correlation networks analysis (WGCNA) allowed identification of coexpressed hub genes with possible main regulatory functions and major impacts on the phenotype. Among those identified, we clarified the role of *CBF4*. This gene showed contrasting expression profiles in the two clones under NAC, being induced in cold-tolerant cmm1T but suppressed in susceptible cmm6-6. By contrast, under AC, *CBF4* was upregulated in both clones. Our study provides a global understanding of mechanisms involved following exposure to NAC and AC in *S. commersonii*. The mechanisms described here will inform future investigations for detailed validation in studies regarding cold tolerance in plants.

1 | INTRODUCTION

The cultivated potato (*Solanum tuberosum* L.) suffers from several abiotic constraints that affect its growth and productivity (Minhas, 2012; Obidiegwu et al., 2015). Among these, cold stress, including chilling (0–10 °C) and freezing (<0 °C),

Abbreviation: AC, acclimated conditions; DEG, differentially expressed gene; FC, fold-change; GBS, genotype-by-sequencing; GO, gene ontology; LT50, 50% lethal injury; MM, module membership; NAC, nonacclimated conditions; qRT-PCR, quantitative real-time polymerase chain reaction; RNA-seq, RNA sequencing; SNP, single nucleotide polymorphism; WGCNA, unsigned weighted correlation networks analysis.

is among the more harmful suboptimal conditions for the cultivated potato, a frost-sensitive crop. Enhanced tolerance to cold stress provides a promising avenue for reducing production losses and increasing the cultivation area, especially important in light of a rapidly growing world population. To date, little progress has been made toward the release of tolerant varieties. This is a result of various reasons, including the polyploid genetics of the tetraploid ($2n = 4x = 48$) cultivated potato, the narrow genetic base for cold tolerance within the cultivated potato gene pool, and the relatively poor comprehension of cold stress mechanisms that would provide efficient breeding targets. Fortunately, cultivated potato is related to a large number of tuber-bearing *Solanum* species. Many of these wild relatives have genes controlling both abiotic and biotic stress tolerance; since these genes are often lacking in cultivated potato, wild potato represents a reservoir of allelic variability to improve noteworthy traits. So far as it is known, *S. commersonii* is one of the most tolerant to low temperatures among wild potato species. It also possesses the best capacity to cold acclimate (i.e., increase its cold tolerance after exposure to low, nonfreezing temperatures) (Palta & Simon, 1993). Stone et al. (1993) provided evidence that cold tolerance and cold acclimation are independent and under polygenic control. Importantly, the genome sequence of *S. commersonii* is available (Aversano et al., 2015), making this species an attractive model to study molecular dynamics and mechanisms underlying cold tolerance and acclimation capacity. Several reports have been published documenting that low-temperature tolerance is a complex process, involving changes in the expression of numerous cold-responsive (*COR*) genes, mainly regulated by the *CBF* cold-response pathway (Chinnusamy et al., 2010; Esposito et al., 2019a). Following microarray analyses, Carvallo et al. (2011) reported distinct *S. commersonii* and cultivated potato *CBF* regulons (genes regulated by *CBFs*). The authors found that the overexpression of *AtCBF3* activates 160 cold-related genes in *S. commersonii* and only 54 in cultivated potato. This finding suggests that differences in cold regulatory programs may explain the distinctness of these two species' freezing tolerance. However, the conclusions drawn by the authors are biased by nucleotide mismatch between *S. commersonii* transcripts and cultivated potato expressed sequence tag probes (Carvallo et al., 2011). Further, microarray experiments are limited in the range of detection and present difficulties in comparing expression levels across different experiments. Next-generation sequencing technologies represent an improvement, allowing sequencing of entire transcriptomes (RNA-seq) as demonstrated for tomato (*Solanum lycopersicum* L.), wheat (*Triticum aestivum* L.), rice (*Oryza sativa* L.), and many other crop species (Da Maia et al., 2017; De Palma et al., 2019; Iquebal et al., 2019; Thomas et al., 2019). Despite the substantial power of RNA-seq to reveal transcriptome perturbations, the approach still has some limitations, especially in identifying coexpressed hub genes that may have main regulatory functions and major impacts on phenotypes. This largely is due to the huge amount of data that RNA-seq studies produce, presenting an analytical, organizational, and interpretive challenge. Weighted gene correlation network analysis (WGCNA) is emerging as an efficient and effective tool to elucidate biological networks and predict individual gene functional role. The approach has been used to study flower development in *Arabidopsis thaliana* (L.) Heynh. (Xie et al., 2015), endosperm development in wheat (Pfeifer et al., 2014), soybean [*Glycine max* (L.) Merr.] domestication (Lu et al., 2016) and blood transcriptome of ewes following hemp seed supplementation in their diet (Iannaccone et al., 2019). It also helped researchers to reveal stress-related genes in rice (Sircar & Parekh, 2015; Zhu et al., 2019) and barrel clover (*Medicago truncatula* Gaertn.) (Burks & Azad, 2016). In the current study, we resorted to RNA-seq and WGCNA to analyze gene expression patterns of two clones of *S. commersonii* contrasting in their cold response, namely cmm1T and cmm6-6. Cmm1T displays a high freezing tolerance (LT50 = −6.4 ˚C), whereas cmm6-6 is cold sensitive (LT50 = −2.8 ˚C) (Carputo et al., 2013) Conversely, both cmm1T and cmm6-6 exhibit a common ability to cold acclimate as, after 2 wk of acclimatization at 4 ˚C, their killing temperatures drop down to −8.9 and −6.7 ˚C, respectively (Carputo et al., 2007, 2013). The findings described in this work contribute to a better understanding of the molecular and physiological mechanisms involved in cold response in *S. commersonii*. Our study provides a list of target genes that might be used in future biotechnological approaches for efficient exploitation of the wide genetic background of wild potato to improve the current breeding strategies of cultivated potato.

Core Ideas

- Differences in expression patterns of two *Solanum* clones contrasting in their cold response.
- WGCNA identifies candidate genes associated with cold tolerance under NAC and AC.
- We documented the role for a *CBF*-dependent pathway under both AC and NAC.

2 | MATERIALS AND METHODS

2.1 | Plant materials and determination of DNA diversity

In our experiment, we used two different genotypes of *S. commersonii*: cmm1T (a clone of PI243503) and cmm6-6 (a clone of PI590886). The former is freezing tolerant and able to cold acclimate. The latter is freezing susceptible but retains capacity to cold acclimate (Carputo et al. 2013). Both clones

were provided as seed by the Inter-Regional Potato Introduction Project (IR-1), Sturgeon Bay, WI (USA). Plants of each clone were maintained in vitro on Murashige and Skoog (MS) medium (Sigma-Aldrich, http://www.sigmaaldrich.com) with 1% (w/v) sucrose and 0.8% (w/v) agar, at 24 ˚C with irradiance of 200 µmol m^{-2} s^{-1}, under a 16/8 h (light/dark) photoperiod. To investigate the genetic diversity underlying the phenotypic differences between cmm1T and cmm6-6, a genotype-by-sequencing (GBS) approach was implemented. One microgram of genomic DNA of each clone extracted through TRIZOL was digested with *ApeKI* and incubated at 37 ˚C for 16–20 h. Fragmented DNA was then purified with Agencourt AMPureXP beads (Beckman Coulter) and ligated to barcoded adapters. Samples were pooled, and the libraries were created using the TruSeq indexes kit (Illumina). The resulting libraries were checked with both Qubit 2.0 Fluorometer (Invitrogen) and Bioanalyzer DNA assay (Agilent Technologies). Libraries were finally processed with Illumina cBot for cluster generation on the flow cell, following the manufacturer's instructions and sequenced with V4 chemistry paired-end 50 bp mode on the HiSeq2500 instrument (Illumina). Once produced, Illumina reads were mapped to the reference genome through BWA-MEM-0.7.10. Duplicated reads were removed using MarkDuplicate implemented in Picard (http://broadinstitute.github.io/picard) and a variant calling was run using Freebayes-0.9.18 with default parameters (Garrison & Marth, 2012).

2.2 | Cold-stress treatment

The cold-stress experiment was performed in 2019 and described by Esposito et al. (2020a). Briefly, 4-wk-old in vitro plantlets were transplanted into 14-cm pots filled with sterile soil and grown for 2 wk in a growth chamber under cool white fluorescent lamps (350–400 µmol m^{-2} s^{-1}) at 24 ˚C (16/8 h light/dark) prior to submitting them to cold stress under either NAC or AC, In particular, in NAC experiments, three plants of each clone were challenged for 30 min at −2 ˚C, while three control plants were kept at 24 ˚C. In AC experiments, six plants per clone were acclimated at 4 ˚C for 2 wk. Then, three were transferred to −2 ˚C for 30 min, while the others, used as controls, were kept at 4 ˚C, as also reported by Iovene et al. (2004). In both experiments, an environmentally controlled cold room was used. At the end of each stress, young leaf samples were collected from all replicates and control plants and individually stored at −80 ˚C.

2.3 | RNA extraction and sequencing

For each sample, total RNA was isolated from leaf tissues using the Spectrum Plant Total RNA kit (Sigma-Aldrich) according to the manufacturer's protocol. The RNA concentrations were determined using a NanoDrop ND-1000 spectrophotometer (Thermo Scientific), and its integrity was verified using a bioanalyzer (Agilent Technologies). Three micrograms of total RNA of each sample were sent to UMN Genomic Center (University of Minnesota, USA) for library preparation. Twenty-four cDNA libraries (three biological replicates from leaves from control and stress conditions for both experiments) were subsequently sequenced using the Illumina HiSeq 2500 sequencing platform, providing 125 bp paired-end reads and a total of 30 million reads per sample, as described by Galise et al. (2021). Sequence quality assessment was carried out using the FASTQC tool version 0.10.0 (http://www.bioinformatics.babraham.ac.uk/projects/fastqc). Trimming was performed using Trimmomatic-0.3330 (Bolger et al., 2014).

2.4 | RNA-seq data analysis and validation

All sequence data sets were loaded into the Artificial Intelligence RNA-seq (AIR) online tool (Vara et al., 2019), and a new RNA-seq experiment was chosen. Gene expression levels were calculated using geometric normalization and the per-condition dispersion method by quantifying the Illumina reads according to the fragments per kilobase per million mapped fragments (FPKM). These values were then used to perform a principal component analysis and to validate biological replicates (Supplemental Figure S1). Fold-changes (FCs) were reported as the log (base 2) of normalized read count abundance for the cold-stressed samples divided by the read count abundance of the control samples. Gene ontology (GO) terms were examined with AgriGO (http://bioinfo.cau.edu.cn/agriGO/) with the following parameters: hypergeometric statistical test method, multi-test adjustment Hochberg false discovery rate, significance level < .05, and three minimum number of mapping entries. Significant values were sorted by enrichment score (Query_item/Query_total)/(Background_item/Background_total) and GO redundancy was removed with the REVIGO tool (http://revigo.irb.hr). MAPMAN software was also used to further understand the biological role of differentially expressed genes (DEGs). Since a physical map for *S. commersonii* is not available yet, we used the Mercator online tool to associate *S. commersonii* proteins to MapMan bins. Then, the list of DEGs was mapped to MapMan bins for data visualization and pathway analysis. Finally, to validate the reliability of the expression profiles observed in the RNA-seq data, 10 genes were used for quantitative real-time PCR (qRT-PCR) analyses using the iTaq SYBR Green supermix (Bio-Rad). Gene-specific primers, designed by Primer3 are listed in Supplemental Table S1. The elongation factor gene *EF* was used as an internal control (Nicot et al., 2005). The

same RNA samples employed subjected to RNA-seq were used as template for this validation. A 2-µl aliquot of 1/10 cDNA, 0.3 µM of each specific primer, and the FAST SYBR Green master mix (Applied Biosystems) comprised a final qRT-PCR volume of 20 µl. The qRT-PCR analyses were performed using an ABI 7900HT Real-Time PCR System (Applied Biosystems), and the relative expression value was calculated through the ΔΔCt method (Livak & Schmittgen, 2001).

2.5 | Unsigned weighted correlation networks analysis

Unsigned weighted correlation networks analysis was used to perform the hierarchical clustering and to identify coexpressed genes (hub genes), which may have main regulatory functions and significant impacts on genes conditioning phenotypes. In detail, four different adjacency matrices (cmm1T and cmm6-6, each under NAC and AC) were created using all expression values (FPKM). The pickSoftThreshold () function was used to choose the proper soft-thresholding power (Langfelder & Horvath, 2008; Langfelder et al., 2011). In particular, for each analysis, the lowest power for which the scale-free topology fit index reaches 0.90 was used (Supplemental Figure S2). The weighted adjacency matrices were then transformed into a topological overlap matrix, which allows the calculation of dissimilarity values used to minimize spurious associations effects. The result was used as input for the linkage hierarchical clustering, and the modules (clusters of highly interconnected genes) were identified in the resulting dendrogram through a dynamic hybrid tree cutting algorithm (DynamicTreeCut algorithm). Finally, we estimated the relationships between each module and the temperature causing 50% lethal injury (LT50) in both clones by calculating the Pearson's correlation using the module eigengene values.

3 | RESULTS

3.1 | Plant material genotyping

To sample the global genetic diversity of cmm1t and cmm6-6, we assayed the DNA sequence variation on a genome-wide scale via GBS. Overall, we identified 16,491 heterozygous variants (GT = 0/1) (single nucleotide polymorphisms [SNPs] and insertion–deletion markers) in cmm1T and 17,186 in cmm6-6. Most of the heterozygous variants (13,413) were in common, whereas 2,708 were private in cmm1T and 3,279 in cmm6-6 (Supplemental Figure S3A). By contrast, 6,841 in the former and 7,863 in the latter were homozygous for the altered allele (GT = 1/1). Among them, 3,891 were in common, 2,456 were private in cmm1T, and 3,602 were in cmm6-6 (Supplemental Figure S3B). Eight hundred sixty-four common variants presented a different genotype, being homozygous in cmm1T but heterozygous in cmm6-6 (494) and vice-versa (370). Most of the variants mainly were due to transition events, mainly C > T and G > A (Supplemental Figure S3C). Fifty-eight percent of the identified variants were localized in intergenic regions followed by downstream (13.8%) and upstream (11.9%) gene regions (Supplemental Figure S3D). Using cultivated potato as the reference genome (*S. commersonii* chromosomes are not available yet), the average number of total variants in each chromosome was calculated. Variants were widely distributed on all chromosomes, from a minimum of 5,051 SNPs on chromosome 00 to a maximum of 28,420 on chromosome 1 (data not shown).

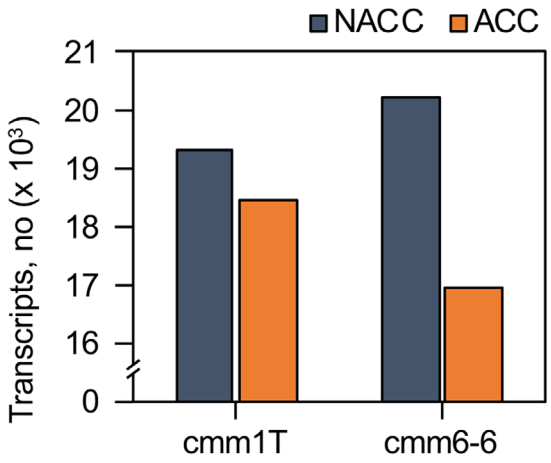

FIGURE 1 Total number of expressed transcripts under nonacclimated (NAC) and acclimated (AC) cold stress conditions in cmm1T and cmm6-6

3.2 | Major differences in transcriptome reprogramming occur in cmm1T and cmm6-6 under NAC

The RNA-seq analysis produced more than one billion reads, with an average of 33 million reads from each sample. A total of 411,579,508 in cmm1T and 414,682,788 in cmm6-6 cleaned reads were obtained in NAC (Supplemental Table S2). Overall, 19,322 and 20,203 transcripts originated from cmm1T and cmm6-6, respectively (Figure 1). Among DEGs, 1,002 and 8,055 were identified in cmm1T and cmm6-6, including 797 (80%) and 4,537 (56%) upregulated genes and 205 (20%) and 3,517 (44%) downregulated, respectively (Figure 2a; Supplemental Table S3). Out of all, 761 DEGs were common between the two clones, whereas 241 were unique to cmm1T and 7,294 to cmm6-6 (Figure 2b). Enrichment analysis of all DEGs was performed to increase the likelihood of correctly assigning their roles to significant common

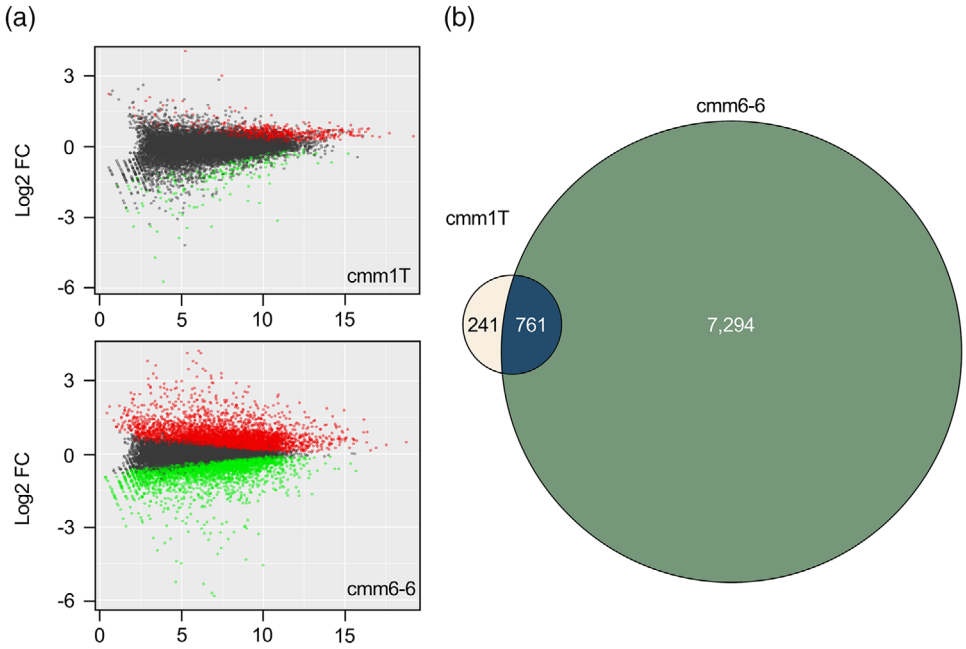

FIGURE 2 Gene response results following 30 min of cold treatment at −2 ˚C under nonacclimated conditions (NAC). (a) Number of total differentially expressed genes (DEGs) in cmm1T and cmm6-6. (b) DEGs that were in common or uniquely expressed

pathways. Approximately 180 and 1,160 unique enriched GO terms were associated with significantly upregulated or downregulated genes in cmm1T and cmm6-6, respectively (Supplemental Tables S4 and S5). The lipid biosynthetic metabolism term applied to DEGs from cmm6-6 but not those from cmm1T, whereas lignin catabolic and biosynthetic processes and regulation of plant type secondary cell wall biogenesis terms were mostly enriched in the cold-tolerant cmm1T rather than in susceptible cmm6-6. In addition, in both cmm1T and cmm6-6, the RNA regulation bin included many DEGs. Among transcription factors belonging to the *ap2/ERF* family, we observed that *CBF3* and *CBF4* were upregulated in cmm1T (FC = 4.2 and 2.7, respectively) but downregulated in cmm6-6 (FC = −2.2 and −3.5). We looked for possible variants within the promoter region to explain the contrasting expression response of the two clones. The GBS data analysis did not provide evidence of polymorphisms within the *CBF3* and *CBF4* promoters (data not shown), although we cannot exclude that our approach did not cover these regions. To further confirm the RNA-seq results, we performed qRT-PCR expression analyses on 10 genes (*CBF1*, *CBF2*, *CBF3*, *CBF4*, *HOS1*, *ZAT12*, *SIZ1*, *CIPK17*, *CIPK23*, and *COR47*) chosen among the main regulators involved in the cold-stress pathway (Table 1). The FCs detected by qRT-PCR were consistent with the expression means inferred from sequencing reads analysis (Table 1). For example, *CBF3*, *CBF4*, and *ZAT12* were induced in cmm1T but repressed in cmm6-6. By contrast, *HOS1*, known to mediate ubiquitination and subsequent proteasomal degradation of the activator *ICE1*, was downregulated in cmm1T but induced in cmm6-6. *SIZ1* was repressed in both clones. No significant changes were found for *CBF1*, *CBF2*, *CIPK17*, *CIPK23*, and *COR47*.

3.3 | Modest differences in transcriptome reprogramming occur in cmm1T and cmm6-6 under AC

Cold stress under AC resulted in 408,578,084 in cmm1T and 406,660,312 in cmm6-6 cleaned reads (Supplemental Table S2). A total of 18,471 and 16,947 transcripts were recovered for cmm1T and cmm6-6, respectively (Figure 1), of which 5,650 and 8,936 were DEGs (Figure 3a; Supplemental Table S6). As was true under NAC, cmm1T yielded a lower number of DEGs than cmm6-6 under AC. Specifically, 2,774 (49%) vs. 4,090 (46%) of upregulated DEGs and 2,876 (51%) vs. 4,846 (54%) of downregulated DEGs originated from cmm1T and cmm6-6, respectively (Figure 3a). Approximately 3,000 DEGs were common between the two clones, whereas 2,642 were unique to cmm1T and 5,928 to cmm6-6 (Figure 3b). One thousand nine and 1,298 unique GO terms were associated with the significantly upregulated or downregulated DEGs in cmm1T and cmm6-6, respectively (Supplemental Tables S7 and S8). Similar terms were enriched in each clone. For example, categories such as ‘cellular process’, ‘biosynthetic process’, ‘primary metabolic process’, ‘response to stress’, ‘response to stimuli’, and “transport" were enriched in both clones (data not shown). Under AC, some *ap2/ERF* transcription factors were enriched in both clones. In particular, *CBF3* and *CBF4* were upregulated in both cmm1T and

TABLE 1 RNA sequencing (RNA-seq) results confirmed by quantitative real-time PCR (qRT-PCR) in cmm1T and cmm6-6 under nonacclimated conditions (NAC) (upregulated) and acclimated conditions (AC) (downregulated) conditions

Condition (*gene*)	CMM1T			CMM6-6		
	RNA-seq (log_2FC)[a]	qPCR-RT (log_2FC)	FDR[b]	RNA-seq (log_2FC)	qPCR-RT (log_2FC)	FDR
Nonacclimated condition						
CBF1	ns[a]	ns	–	ns	ns	–
CBF2	ns	ns	–	ns	ns	–
CBF3	4.2	3.5	0.018	−2,23	−1	0.008
CBF4	2.7	2	0.047	−3,5	−2,7	9.9×10^{-16}
HOS1	−1,2	−1	0.039	1,8	0,8	0.006
SIZ1	−2.5	−1	0.036	−4	−3	0.022
ZAT12	2	1.7	0.040	−2,8	−2	0.0016
CIPK17	ns	ns	–	ns	ns	–
CIPK23	ns	ns	–	ns	ns	–
COR47	ns	ns	–	ns	ns	–
Acclimated condition						
CBF1	ns	ns	–	ns	ns	–
CBF2	ns	ns	–	ns	ns	–
CBF3	2.8	2.4	0.018	3.3	2.5	0.019
CBF4	2.1	1.9	0.019	2.3	1.6	1.1×10^{-16}
HOS1	−2.9	−1.8	0.046	−2.2	−1.4	0.047
SIZ1	−0.8	−0.4	0.041	−1	−0.5	0.037
ZAT12	2.8	1.9	0.035	3	2.2	2.1×10^{-14}
CIPK17	ns	ns	–	ns	ns	–
CIPK23	ns	ns	–	ns	ns	–
COR47	ns	ns	–	ns	ns	–

[a]FC, fold changes.
[b]False discovery rate.
[c]Not significant.

cmm6-6 (FC = 2.8 and 3.3, respectively), further underlying their potential role in cold-acclimation processes. For both genes, the expression values obtained via qRT-PCR were comparable to RNA-seq data (Table 1). *ZAT12* was induced in both clones, whereas *HOS1* and *SIZ1* were repressed. No significant changes were found for *CBF1*, *CBF2*, *CIPK17*, *CIPK23*, and *COR47*. Notably, in both cmm1T and cmm6-6, 38% of DEGs were assigned to an unknown functions, suggesting that many of the genes involved in cold tolerance following acclimation have yet to be fully described. Genotype-specific modules, such as secondary metabolism in cmm1T and response to abiotic stress in cmm6-6, were also identified.

3.4 | WGCNA identifies potential candidate genes associated with cold tolerance under NAC and AC

Under NAC, WGCNA analysis identified 26 different highly coexpressed clusters of genes (modules) in both clones (Figure 4a). The largest module (turquoise in both cmm1T and cmm6-6) consisted of 8,851 and 5,246 genes, whereas the smallest (darkgrey in both cmm1T and cmm6-6) contained 45 and 128 genes, respectively (Supplemental Table S9). The salmon cluster ($r = 0.64$) in cmm1T and the purple ($r = 0.72$) in cmm6-6 were correlated with the stress-tolerance phenotype (Figure 4a). For both modules, we focused on the genes with the highest intramodular connectivity (hub genes, module membership [MM] > 0.65), as these genes may represent points of biological interest in defining our phenotypes (Figure 4b). Eighty-three genes belonging to the salmon module in cmm1T (MM > 0.65) were involved in RNA regulation, lignin biosynthesis, lipid metabolism, stress-responsive genes, and protein transport (Supplemental Table S10). Among those involved in RNA regulation, the *AP2/ERF* gene family was highly associated with cold tolerance in cmm1T (data not shown). Genes involved in the phenylpropanoid-lignin biosynthetic pathway (i.e., *HCT*, *C3H*, *F5H*, *LAC4*, and *PRX72*) also clustered in the salmon group and were all downregulated in cmm1T. These data

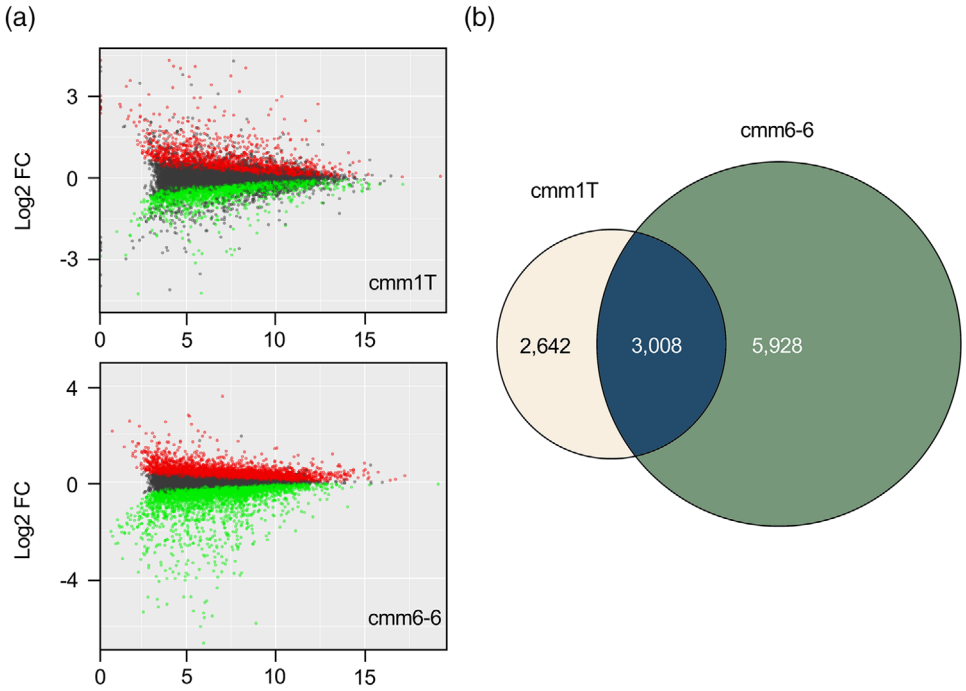

FIGURE 3 Gene response results following 30 min of cold treatment at −2 ˚C under acclimated conditions (AC). (a) Number of total differentially expressed genes (DEGs) in cmm1T and cmm6-6. (b) DEGs in common or uniquely expressed

agree with GO enrichment analysis, where lignin catabolic and biosynthetic processes and plant type secondary cell wall biogenesis terms were particularly enriched in the cold-tolerant cmm1T rather than in the cold-sensitive cmm6-6 (data not shown). Additionally, an acyl carrier protein (ACP) involved in fatty acid biosynthesis was also found in the same salmon module and was significantly induced. The cmm6-6 purple included 821 genes (MM > 0.65; Figure 4b) involved in DNA repair, DNA synthesis, chromatin organization, and protein activation and degradation (Supplemental Table S10). Although WGCNA analysis clarifies the role of some genes involved in cold-stress tolerance, further studies are needed to investigate DEGs for which descriptions and GO terms are unknown.

Under AC, all genes were grouped in 27 and 30 modules in cmm1T and cmm6-6, respectively (Figure 5a). The largest module (turquoise in both cmm1T and cmm6-6) consisted of 4,525 and 6,748 genes, respectively, whereas the smallest (orange in cmm1T and skyblue in cmm6-6) contained 37 and 74 genes, respectively. The module–trait relationships revealed that temperature causing LT50 under AC was correlated with the royal blue cluster in cmm1T (r = 0.89), the light cyan cluster in cmm6-6 (r = 0.81), and the red module in both clones (r = 0.72 in cmm1T and r = 0.77 in cmm6-6) (Figure 5a). The cmm1T specific module royal blue contained 198 genes (Supplemental Table S9). Among them, a gene involved in secondary metabolisms (an acyl-transferase similar to *AT2G39980*) was identified. By contrast, the cmm6-6 specific module light cyan had 299 genes (Supplemental Table S9) including a heat-shock transcription factor (*HSFs*) similar to *AtHSFA4C* and a stress-responsive gene similar to *RESPONSIVE TO DEHYDRATION22* (*AtRD22*). Since cmm1T and cmm6-6 are both able to cold acclimate, we examined the shared red module genes. The red cluster comprises 1,320 genes in cmm1T and 1,216 in cmm6-6 (Figure 5b). Out of 53 common genes, 36 had known annotations. Most were involved in RNA regulation, protein synthesis and modifications, and miscellaneous functions (Supplemental Table S10). Notably, *CBF3* and *CBF4* (MM > 0.65) were located in this module and both were induced in cmm1T and cmm6-6. Two additional key transcription factors involved in the modulation of cold-related genes were identified in this coexpression network (MM > 0.65): a MYB-related (similar to *AT3G04030*, *MYR2*) and a WD-40 protein (similar to *AT5G67320*, *HOS15*) involved in histone deacetylation in response to abiotic stress.

4 | DISCUSSION

In potato, exposure to cold represents an abiotic stress that can significantly impact crop growth, yield, and economics. While the cultivated gene pool for potato lacks much diversity for cold tolerance, some wild potato species, most notably *S. commersonii*, harbor genes for both cold tolerance and cold acclimation, which, therefore, makes it a species of interest to potato breeders and provides a tractable system to study the regulation of cold adaptation. Here we described, for the

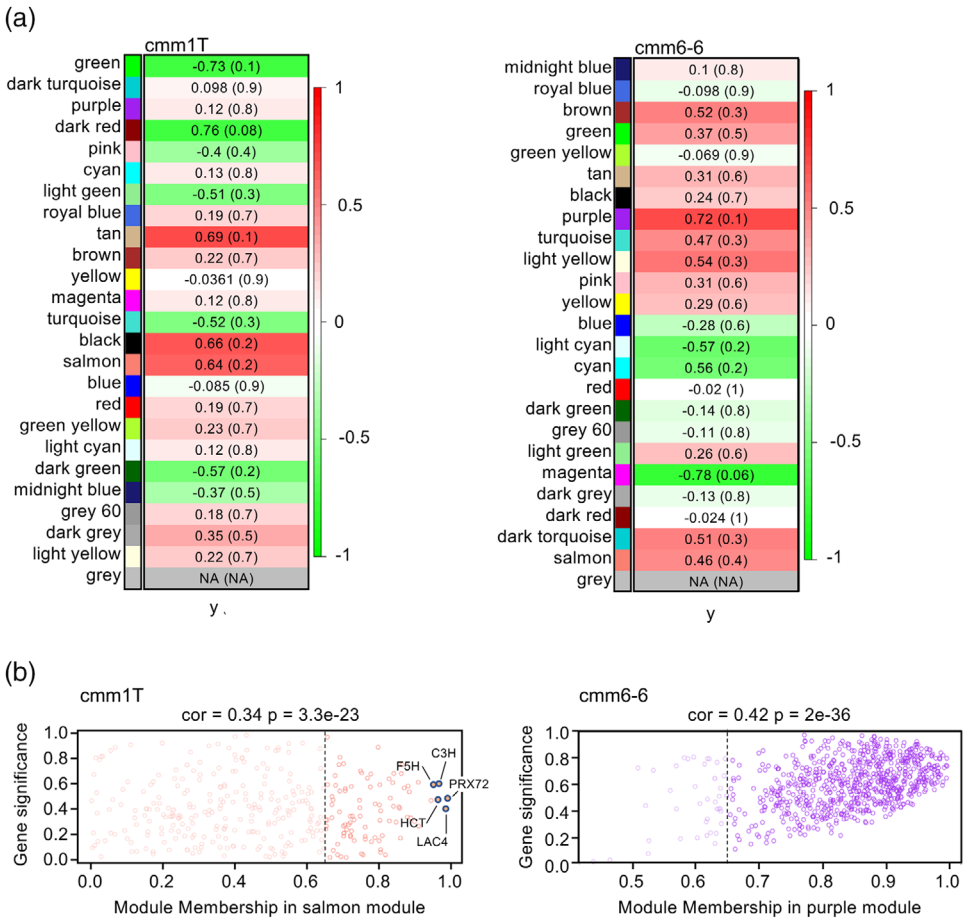

FIGURE 4 Composite visualization of coexpression analysis under nonacclimated conditions (NAC). (a) Modules–trait association plots showing module eigengenes associated with the trait in cmm1T and cmm6-6. Each row corresponds to different modules (labeled by color): green represents low adjacency (negative correlation); red represents high adjacency (positive correlation). (b) Scatterplot gene significance for weight (GS) vs. module membership (MM) for the salmon module in cmm1T and the purple module in cmm6-6. Genes showing MM > 0.65 are reported on the right of the dashed line

first time, the transcriptomic response of two *S. commersonii* clones contrasting in cold tolerance but both are able to cold acclimate. We further analyze the molecular mechanisms involved in cold tolerance and cold acclimation.

4.1 | Coexpression network analysis reveals major differences in transcriptome reprogramming of NAC-stressed cmm1T and cmm6-6

Our analysis indicated that most of cmm1T-specific genes in the salmon module (correlated with the phenotypic trait) were involved in lignin synthesis and modifications, lipid metabolism, stress responsive genes, and protein transport. For example, a laccase (similar to *AtLAC4*, *AT2G38080*), which is involved in lignin biosynthesis, was found suppressed in cmm1T. Gall et al. (2015) reported that reduction in lignin deposition in cell walls not only increases its permeability but also enhances its elasticity. Recently, we also showed that other *LAC* genes, such as *LAC3*, *LAC12*, and *LAC13*, were repressed by microRNAs (miRNA408) under NAC, confirming that a fine-tuning expression of laccases is important to determine cold tolerance in cmm1T (Esposito et al., 2020a, 2020b). These features may allow cell walls to withstand growing ice crystals, thus reducing damages. *AtPRX72*, which encodes a peroxidase, was reported by Herrero et al. (2013) to be implicated in lignin biosynthesis. Consistent with the possibility that lignin deposition is reduced under cold stress, our analyses discovered a differentially expressed peroxidase gene similar to *AtPRX72*, the suppression of which in cmm1T was significantly associated with the cold tolerance. By contrast, an aspartic protease gene (similar to *ASPG1-OE*), which encodes a protein associated with the endomembrane system, was induced in cmm1T. Yao et al. (2012) showed that water loss was dramatically reduced in *Arabidopsis* mutant lines ectopically overexpressing the *ASPG1-OE*. Presumably, accumulation of aspartic protease

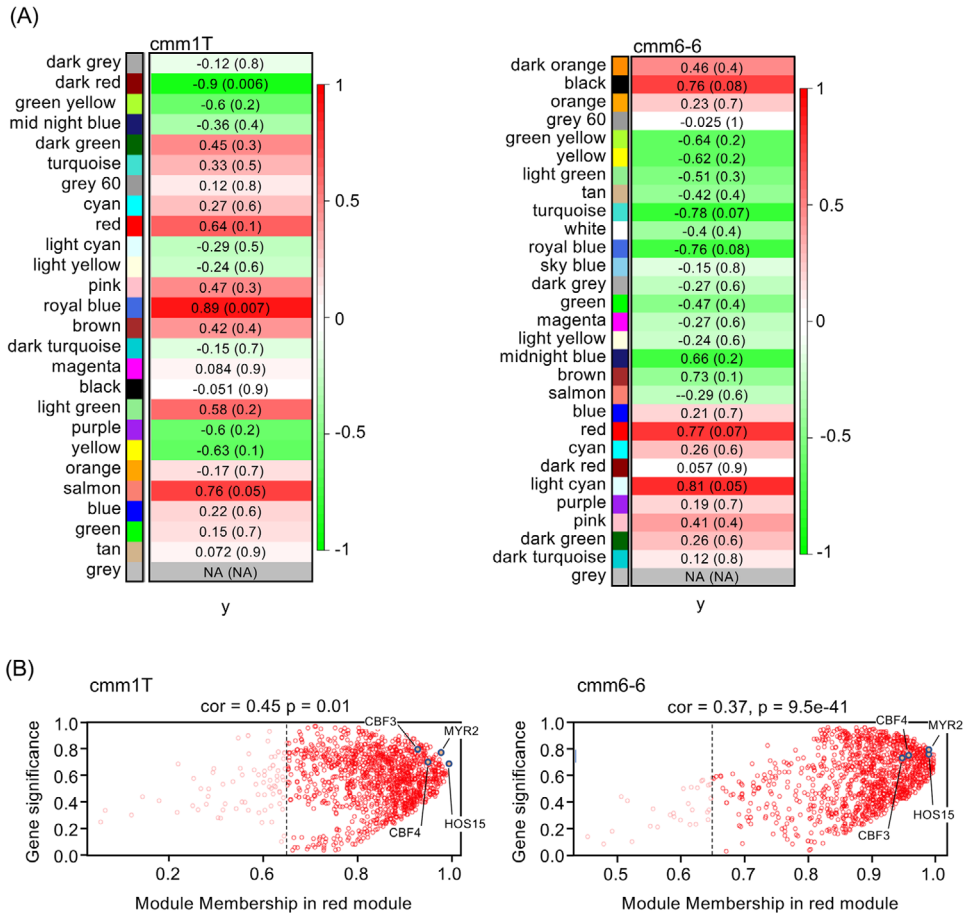

FIGURE 5 Composite visualization of coexpression analysis under acclimated conditions (AC). (a) Modules–trait association plots showing module eigengenes associated with the trait in cmm1T and cmm6-6. Each row corresponds to different modules (labeled by color): green represents low adjacency (negative correlation); red represents high adjacency (positive correlation). (b) Scatterplot of gene significance for weight (GS) versus module membership (MM) for the red module in cmm1T and cmm6-6. Genes showing MM > 0.65 are reported on the right of the dashed line

results in reduced free water that might be transformed into ice, which in turn can rupture the plasmatic membrane. Also induced in cmm1T was the acyl carrier protein gene (*ACP*), which encodes an essential cofactor carrying acyl chains of different lengths. Acyl carrier protein participates in cycles of condensation, reduction, and dehydration. Evidence from in vitro and in vivo studies indicated that ACP isoforms are specific for enzymes involved in fatty acid biosynthesis, suggesting that they act by changing the fatty acid composition of cell membranes and leaves (Huang et al., 2017). Tang et al. (2012) confirmed a link between *ACP* and cold tolerance in transgenic tobacco (*Nicotiana tabacum* L.) lines overexpressing the *ACP* gene. Notably, GO terms associated with these *ACP* processes were not found for the cold-sensitive clone cmm6-6. Also noteworthy are genes involved in RNA regulation. Two transcription factors, *CBF3* and *CBF4*, were differentially expressed and induced in cmm1T. These genes were also responsive in cmm6-6 but with contrasting kinetics, suggesting a different regulation of *CBF* genes in the two clones. Compared with *CBF3* and *CBF4*, *CBF1* and *CBF2* did not change their expression following NAC in both clones. This agrees with the theory that the induction of *CBF3* may repress the expression of *CBF2*. Our data are also consistent with Novillo et al. (2004), who reported that *CBF2* negatively regulates the expression of *CBF1* and *CBF3* in *Arabidopsis*. The *CBF* genes are key players in plant cold tolerance mechanisms. In *Arabidopsis*, three duplicated *CBFs* (*AtCBF1/DREB1b*, *AtCBF2/DREB1c*, and *AtCBF3/DREB1a*) regulate the expression of more than 100 cold responsive (*COR*) genes that impart freezing tolerance (Maruyama et al., 2004; Vogel et al., 2005). In crop plants, *CBF* genes are widely distributed and often duplicated (Knox et al., 2010; Aversano et al., 2015). In *S. commersonii*, in particular, comparative analyses indicated that the *CBF* genes underwent rapid expansion via duplication processes, which led to the presence of four paralogs (*CBF1*, *CBF*2, *CBF*3, and *CBF*4) and two pseudo-genes (*ψCBF2* and *ψCBF3*) arranged in tandem (Aversano et al., 2015). Reports on the functional role of each

CBF in *S. commersonii* are still scanty. Pino et al. (2008) demonstrated that the overexpression of *AtCBF1* in transgenic lines of *S. commersonii* further increases the freezing tolerance in response to low temperature. Later, Carvallo et al. (2011) reported that in transgenic *S. commersonii* and cultivated potato constitutively expressing *AtCBF3*, 160 cold-induced genes were upregulated in the former species and only 54 in the latter. These data reveal a rapid evolution of the *CBF* pathways in the two plant species that may contribute to their freezing tolerance differences.

Besides *CBF* genes, it is worthy to note that other genes involved in the cold signaling pathway were affected in our *S. commersonii* clones. For example, *HOS1*, known to be a negative regulator of the INDUCED CBF EXPRESSION 1 (*ICE1*) gene, was repressed in cmm1T but induced in cmm6-6. This probably explains why *CBF3* and *CBF4* were downregulated in cmm6-6 compared with cmm1T. Taken together, our observations suggest that molecular mechanisms involved in the regulation of cold signaling pathway might explain the contrasting phenotypes of cmm1T and cmm6-6.

4.2 | RNA-seq reveals genotype-specific and common genes associated with cold tolerance under AC

Consistent with their common ability to cold acclimate, cmm1T and cmm6-6 showed similar behavior as indicated by number of DEGs, percentage of up- and downregulated genes and modules detection following acclimation. For example, the red module correlated with the temperature causing LT50 for both clones. In this module, both *CBF3* and *CBF4* (MM > 0.65) were identified and both were induced in cmm1T and cmm6-6; by contrast, *CBF1* and *CBF2* were not affected. A WD-40 protein (similar to *AT5G67320*, *HOS15*) involved in histone deacetylation was also found in the same module. It has been shown that loss of function *Arabidopsis* mutants of this latter gene were hypersensitive to freezing (Zhou et al. 2008). More recently, Park et al. (2018) reported a mechanism of gene derepression through which *HOS15* promotes the degradation of histone deacetylase HD2C in a cold-dependent manner, inducing switches in chromatin structure and facilitating recruitment of *CBF* genes to the *COR* gene promoters. Our results suggest that *HOS15* might be essential for similar activation of *CBF3* and *CBF4* in both cmm1T and cmm6-6 during cold stress under AC. Along with the activation of *HOS15*, the repression of *HOS1* in both clones is also intriguing. It is known that *HOS1* interacts with the cold activator *ICE1*. According to the proposed mechanism, under non-stressful temperatures *HOS1* ensures low levels of *ICE1*; as a consequence, the cold-signaling pathway is not induced. By contrast, in response to cold, the mRNA level of *HOS1* rapidly and transiently decreases, alleviating the *ICE1* degradation; this allows the cold responses through *CBF3* (Lee et al., 2005). We hypothesize that the downregulation of *HOS1* may be important also for the subsequent activation of *CBF4*.

Differences in cold-stress response between the two clones were also identified. Under AC, cmm1T modulates the expression of genes involved in secondary metabolism as revealed by annotation of DEGs and by genes belonging to the royal blue module. Of particular note are upregulated genes involved in anthocyanin production and accumulation, including an acyl-transferase gene (augustus_masked_scaffold6708_abinit_gene_0_10, similar to *AT2G39980*). This observation is consistent with previous observations that phenolic compounds, including flavonoids and especially anthocyanins, are commonly induced by low temperatures (Janska et al., 2010; Kovinich et al., 2014). Anthocyanins are fundamental for plant physiological processes, and their abundance in *S. commersonii* leaves has been associated with a greater tolerance to cold stress (D'Amelia et al., 2017). Our data suggest anthocyanins have positive impacts on cold tolerance in cmm1T and may be acting directly as cell osmoregulators (Chalker-Scott, 2002) and indirectly by enhancing photosynthesis (Steyn et al., 2002). On the other hand, in response to cold stress under AC, cmm6-6 displayed enhanced expression of genes involved in abiotic stress response, RNA regulation, and signaling. Among them, a member of heat-shock transcription factor (*HSFs*) (similar to AT5G45710, *HSFA4C*) showed fivefold up-regulation relative to the control. *HSFs* are transcriptional regulators that mediate the activation of a large set of genes induced by high temperature or other stress conditions. They exist in multiple copies (e.g., 21 genes in *Arabidopsis*, 24 in tomato (Scharf et al., 2012), 27 in desert poplar (*Populus euphratica* Olivier) (Zhang et al., 2016), 40 in upland cotton (*Gossypium hirsutum* L.) (Wang et al., 2014), 27 in shrub willow (*Salix suchowensis* W. C. Cheng) (Zhang et al., 2015), 25 in rice (Scharf et al., 2012), and 56 in wheat (Xue et al., 2014). Wang et al. (2014) revealed remarkable differences in transcriptional regulation of *HSF* genes, concluding that HSF proteins have undergone considerable functional diversification. Among the families identified in *Arabidopsis*, the function of the HSFA4 group is not well known. It has been reported that HSFA4A of wheat and rice increases cadmium tolerance (Shim et al., 2009), whereas HSFA4 from tomato activates heat-stress-induced genes and interacts with HSFA5. In our study, the induction of the *HSFA4C* gene under AC might contribute to the cold tolerance of cmm6-6. Similarly, a related *HSF* gene (similar to *AtRD22*) was induced in cmm6-6. *AtRD22* is induced in response to different stresses including drought and exogenous ABA stress (Harshavardhan et al., 2014). *RD22* has been reported to be upregulated by stress conditions in rice (Ding et al., 2009; Wang et al., 2007) and maize (*Zea mays* L.) (Gan et al., 2011) consistent with an important role in cold-stress response in *S. commersonii*.

5 | CONCLUSION

We report for the first time the global pattern of transcriptomic changes of two clones of *S. commersonii* contrasting in their cold tolerance via RNA-seq. Under NAC, many genes were affected in the cold-susceptible genotype vs. the cold-tolerant genotype. By contrast, both clones showed a similar behavior when first cold acclimated. Using WGCNA to elucidate biological gene networks, we document a pivotal role for a *CBF* pathway under both AC and NAC, although the cold-acclimation and cold-tolerance traits are independently regulated. Particularly interesting was *CBF4*. This gene displayed opposing expression trends (increased vs. decreased expression levels in the tolerant cmm1T vs. sensitive cmm6-6 under NAC, respectively). By contrast, under AC, *CBF4* was induced in both clones. Our results contribute to advanced understanding of the molecular basis of cold response under AC and NAC, facilitating more in-depth analyses of the molecular and physiological mechanisms behind cold tolerance in potato and contributing to future biotechnological applications.

ACKNOWLEDGMENTS

This work was carried out within the project 'Development of potato genetic resources for sustainable agriculture' (PORES) funded by the University of Naples Federico II.

CONFLICT OF INTEREST

The authors declare that there is no conflict of interest.

ORCID

Riccardo Aversano https://orcid.org/0000-0002-4041-3702

Domenico Carputo https://orcid.org/0000-0003-1735-9338

REFERENCES

Aversano, R. Contaldi F., Raffaella Ercolano M., Grosso V., Iorizzo M., Tatino F., Xumerle L., Dal Molin A., Avanzato C., Ferrarini A., Delledonne M., Sanseverino W., Aiese Cigliano R., Capella-Gutierrez S., Gabaldón T., Frusciante L., Bradeen J. M., & Carputo D. (2015). The *Solanum commersonii* genome sequence provides insights into adaptation to stress conditions and genome evolution of wild potato relatives. *Plant Cell*, *27*, 954–968. https://doi.org/10.1105/tpc.114.135954

Bolger, A. M. Lohse M., & Usadel B. (2014). Trimmomatic: A flexible trimmer for Illumina sequence data. *Bioinformatics*, *30*, 2114–2120. https://doi.org/10.1093/bioinformatics/btu170

Burks, D. J., & Azad, R. K. (2016). Identification and network-enabled characterization of auxin response factor genes in *Medicago truncatula*. *Frontiers in Plant Science*, *7*, 1857. https://doi.org/10.3389/fpls.2016.01857

Carputo, D., Alioto, D., Aversano, R., Garramone, R., Miraglia, V., Villano, C., & Frusciante, L. (2013). Genetic diversity among potato species as revealed by phenotypic resistances and SSR markers. *Plant Genetic Resourcing*, *11*, 131–139. https://doi.org/10.1017/S1479262112000500

Carputo, D., Castaldi, L., Caruso, I., Aversano, R., Monti, L., & Frusciante, L. (2007). Resistance to frost and tuber soft rot in near-pentaploid *Solanum tuberosum–S. commersonii* hybrids. *Breeding Science*, *57*, 145–151. https://doi.org/10.1270/jsbbs.57.145

Carvallo, M. A., Pino M. T., Jeknic Z., Zou C., Doherty C. J., Shiu S. H., Chen T. H. H., & Thomashow M. F. (2011). A comparison of the low temperature transcriptomes and CBF regulons of three plant species that differ in freezing tolerance: *Solanum commersonii*, *Solanum tuberosum*, and *Arabidopsis thaliana*. *Journal of Experimental Botany*, *62*, 3807–3819. https://doi.org/10.1093/jxb/err066

Chalker-Scott, L. (2002). Do anthocyanins function as osmoregulators in leaf tissues? *Advances in Botanical Research*, *37*, 103–127. https://doi.org/10.1016/S0065-2296(02)37046-0

Chinnusamy, V., Zhu, J. K., & Sunkar, R. (2010). Gene regulation during cold stress acclimation in plants. *Methods in Molecular Biology*, *639*, 39–55. https://doi.org/10.1007/978-1-60761-702-0_3

da Maia, L. C., Cadore P. R. B., Benitez L. C., Danielowski R., Braga E. J. B., Fagundes P. R. R., Magalhães A. M., & de Oliveira A. C. (2017). Transcriptome profiling of rice seedlings under cold stress. *Functional Plant Biology*, *44*, 419. https://doi.org/10.1071/FP16239

D'Amelia, V., Aversano, R., Ruggiero, A., Batelli, G., Appelhagen, I., Dinacci, C., Hill, L., Martin, C., & Carputo, D. (2017) Subfunctionalization of duplicate *MYB* genes in *Solanum commersonii* generated the cold-induced *ScAN2* and the anthocyanin regulator *ScAN1*. *Plant Cell & Environments*, *41*, 1038–1051. https://doi.org/10.1111/pce.12966

De Palma, M., Salzano, M., Villano, C., Aversano, R., Lorito, M., Ruocco, M., Docimo, T., Piccinelli, A. L., D'Agostino, N., & Tucci, M. (2019). Transcriptome reprogramming, epigenetic modifications and alternative splicing orchestrate the tomato root response to the beneficial fungus *Trichoderma harzianum*. *Horticulture research*, *6*, 5. https://doi.org/10.1038/s41438-018-0079-1

Ding, X., Hou, X., Xie, K., & Xiong, L. (2009). Genome-wide identification of *BURP* domain-containing genes in rice reveals a gene family with diverse structures and responses to abiotic stresses. *Planta*, *230*, 149–163. https://doi.org/10.1007/s00425-009-0929-z

Esposito, S., Aversano, R., Bradeen, J. M., Di Matteo, A., Villano, C., & Carputo, D. (2020a). Deep-sequencing of *Solanum commersonii* small RNA libraries reveals riboregulators involved in cold stress response. *Plant Biology*, *1*, 133–142. https://doi.org/10.1111/plb.12955

Esposito, S., Carputo, D., Cardi, T., & Tripodi, P. (2020b). Applications and trends of machine learning in genomics and phenomics for next-generation breeding. *Plants*, *9*, 34. https://doi.org/10.3390/plants9010034

Esposito, S., D'Amelia, V., Carputo, D., & Aversano, R. (2019). Genes involved in stress signals: The CBLs-CIPKs network in cold tolerant *Solanum commersonii*. *Biologia Plantarum*, *63*, 699–709. https://doi.org/10.32615/bp.2019.072

Galise, R. T., Esposito, S., D'Agostino, N. (2021). Guidelines for setting up a mRNA sequencing experiment and best practices for bioinformatic data analysis. In: Tripodi P. (Ed.), *Crop breeding. Methods in molecular biology* (pp. 137–162). Humana. https://doi.org/10.1007/978-1-0716-1201-9_10

Gall, H., Philippe, F., Domon, J. M., Gillet, F., Pelloux, J., & Rayon, C. (2015). Cell wall metabolism in response to abiotic stress. *Plants*, *4*, 112–166. https://doi.org/10.3390/plants4010112

Gan, D., Jiang, H., Zhang, J., Zhao, Y., Zhu, S., & Cheng, B. (2011). Genome-wide analysis of BURP domain-containing genes in maize and sorghum. *Molecular Biology Reports*, *38*, 4553–4563. https://doi.org/10.1007/s11033-010-0587-z

Garrison, E., & Marth, G. (2012). Haplotype-based variant detection from short-read sequencing. *ArXiv*, *1207*, 3907.

Harshavardhan, V. T., Son L. V., Seiler C., Junker A., Weigelt-Fischer K., Klukas C., Altmann T., Sreenivasulu N., Bäumlein H., & Kuhlmann M. (2014). *AtRD22* and *AtUSPL1*, Members of the plant-specific BURP domain family involved in *Arabidopsis thaliana* drought tolerance. *PLoS ONE*, *9*, e110065. https://doi.org/10.1371/journal.pone.0110065

Herrero, J., Fernández-Pérez F., Yebra T., Novo-Uzal E., Pomar F., Pedreño M. Á., Cuello J., Guéra A., Esteban-Carrasco A., & Zapata J. M. (2013). Bioinformatic and functional characterization of the basic *peroxidase 72* from *Arabidopsis thaliana* involved in lignin biosynthesis. *Planta*, *237*, 1599–1612. https://doi.org/10.1007/s00425-013-1865-5

Huang, J., Xue, C., Wang, H., Wang, L., Schmidt, W., Shen, R., & Lan P. (2017). Genes of acyl carrier protein family show different expression profiles and overexpression of acyl carrier protein 5 modulates fatty acid composition and enhances salt stress tolerance in *Arabidopsis*. *Frontiers Plant Science*, *8*, 987. https://doi.org/10.3389/fpls.2017.00987

Iannaccone, M., Ianni A., Contaldi F., Esposito S., Martino C., Bennato F., Angelis E. D., Grotta L., Pomilio F., Giansante D., & Martino G. (2019) Whole blood transcriptome analysis in ewes fed with hemp seed supplemented diet. *Scientific Reports*, *9*, 16192. https://doi.org/10.1038/s41598-019-52712-6

Iovene, M., Barone, A., Frusciante, L., & Monti, L. (2004). Selection for aneuploid potato hybrids combining a low wild genome content and resistance traits from *S. commersonii*. *Theoretical and Applied Genetics*, *109*, 1139–1146. https://doi.org/10.1007/s00122-004-1741-6

Iquebal, M. A., Sharma P., Singh Jasrotia R., Jaiswal S., Kaur A., Saroha M., Angadi U. B., Sheoran S., Singh R., Singh G. P., Rai A., Tiwari R., & Kumar D. (2019) RNAseq analysis reveals drought-responsive molecular pathways with candidate genes and putative molecular markers in root tissue of wheat. *Scientific Reports*, *9*, 13917. https://doi.org/10.1038/s41598-019-49915-2

Janska, A., Marsik, P., Zelenkova, S., & Ovesna, J. (2010). Cold stress and acclimation–what is important for metabolic adjustment? *Plant Biology*, *12*, 395–405. https://doi.org/10.1111/j.1438-8677.2009.00299.x

Knox, A. K., Dhillon, T., Cheng, H. M., Tondelli, A., Pecchioni, N., & Stockinger, E. J. (2010). *CBF* gene copy number variation at *Frost Resistance-2* is associated with levels of freezing tolerance in temperate-climate cereals. *Theoretical and Applied Genetics*, *121*, 21–35. https://doi.org/10.1007/s00122-010-1288-7

Kovinich, N., KayanJa, G., Chanoca, A., Riedl, K., Otegui, M. S., & Grotewol, D. (2014). Not all anthocyanins are born equal: Distinct patterns induced by stress in *Arabidopsis*. *Planta*, *240*, 931–940. https://doi.org/10.1007/s00425-014-2079-1

Langfelder, P., & Horvath, S. (2008). WGCNA: An R package for weighted correlation network analysis. *BMC Bioinformatics*, *9*, 559. https://doi.org/10.1186/1471-2105-9-559

Langfelder, P., Luo, R., Oldham, M. C., & Horvath, S. (2011). Is my network module preserved and reproducible? *PLoS Computational Biology*, *7*, e1001057. https://doi.org/10.1371/journal.pcbi.1001057

Lee, B. H., Henderson, D. A., & Zhu, J. K. (2005). The *Arabidopsis* cold-responsive transcriptome and its regulation by *ICE1*. *The Plant Cell*, *17*, 3155–3175. https://doi.org/10.1105/tpc.105.035568

Livak, K. J., & Schmittgen, T. D. (2001). Analysis of relative gene expression data using real-time quantitative PCR and the $2^{-\Delta\Delta CT}$ method. *Methods*, *25*, 402–408. https://doi.org/10.1006/meth.2001.1262

Lu, X., Li, Q. T., Xiong, Q., Li, W., Bi, Y. D., Lai, Y. C., Liu, X. L., Man, W. Q., Zhang, W. K., Ma, B., Chen, S. Y., & Zhang, J. S. (2016). The transcriptomic signature of developing soybean seeds reveals the genetic basis of seed trait adaptation during domestication. *The Plant Journal*, *86*, 530–544. https://doi.org/10.1111/tpj.13181

Maruyama, K., Sakuma, Y., Kasuga, M., Ito, Y., Seki, M., Goda, H., Shimada, Y., Yoshida, S., Shinozaki, K. & Yamaguchi-Shinozaki, K. (2004). Identification of cold-inducible downstream genes of the Arabidopsis DREB1A/ CBF3 transcriptional factor using two microarray systems. *Plant Journal*, *38*, 982–993. https://doi.org/10.1111/j.1365-313X.2004.02100.x

Minhas, J. S. (2012). Potato: Production strategies under abiotic stress. In N. Tuteja, S. S. Gill, A. F. Tiburcio, R. Tuteja (Eds.), *Improving crop resistance to abiotic stress* (pp. 1155–1167) Wiley-VCH Verlag GmbH & Co. KGaA. https://doi.org/10.1002/9783527632930.ch45

Nicot, N., Hausman, J. F., Hoffmann, L., & Evers, D. (2005). Housekeeping gene selection for real-time RT-PCR normalization in potato during biotic and abiotic stress. *Journal of Experimental Botany*, *56*, 2907–2914. https://doi.org/10.1093/jxb/eri285

Novillo, F., Alonso, J. M., Ecker, J. R., & Salinas, J. (2004). *CBF2/DREB1C* is a negative regulator of *CBF1/DREB1B* and *CBF3/DREB1A* expression and plays a central role in stress tolerance in *Arabidopsis*. *Proceedings of the National Academy of Sciences of the United States of America*, *11*, 3985–3990. https://doi.org/10.1073/pnas.0303029101

Obidiegwu, J., Bryan, G., Jones, G., & Prashar, A. (2015). Coping with drought: Stress and adaptive responses in potato and perspectives for improvement. *Frontiers in Plant Science*, *6*, 542. https://doi.org/10.3389/fpls.2015.00542

Palta, J. P., & Simon, G. (1993). Breeding potential for improvement of freezing stress resistance: Genetic separation of freezing tolerance, freezing avoidance, and capacity to cold acclimate. In P.H. Li (Ed.) *Advances in plant cold hardiness* (pp. 299–310). CRC Press.

Park, J., Lim C. J., Shen M., Park H. J., Cha J. Y., Iniesto E., Rubio V., Mengiste T., Zhu J. K., Bressan R. A., Lee S. Y., Lee B. H., Jin J. B., Pardo J. M., Kim W. Y., & Yun D. J. (2018). Epigenetic switch from repressive to permissive chromatin in response to cold stress. *Proceedings of the National Academy of Sciences U.S.A*, *115*, 5400–5409. https://doi.org/10.1073/pnas.1721241115

Pfeifer, M., Kugler K. G., Sandve S. R., Zhan B., Rudi H., Hvidsten T. R., Mayer K. F. X., & Olsen O. A., International Wheat Genome Sequencing Consortium (2014). Genome interplay in the grain transcriptome of hexaploid bread wheat. *Science*, *345*, 1250091. https://doi.org/10.1126/science.1250091

Pino, M. T., Skinner, J. S., Park, E. J., Jeknić, Z., Hayes, P. M., Thomashow, M. F., & Chen, H. (2008). Use of a stress inducible promoter to drive ectopic *AtCBF* expression improves potato freezing tolerance while minimizing negative effects on tuber yield.

Plant Biotechnology Journal, *5*, 591–604. https://doi.org/10.1111/j.1467-7652.2007.00269.x

Scharf, K. D., Berberich, T., Ebersberger, I., & Nover, L. (2012). The plant heat stress transcription factor (Hsf) family: Structure, function and evolution. *Biochimica et Biophysica Acta*, *1819*, 104–119. https://doi.org/10.1016/j.bbagrm.2011.10.002

Shim, D., Hwang J. U., Lee J., Lee S., Choi Y., An G., Martinoia E., & Lee Y. (2009). Orthologs of the class A4 heat shock transcription factor *HsfA4a* confer cadmium tolerance in wheat and rice. *Plant Cell*, *21*, 4031–4043. https://doi.org/10.1105/tpc.109.066902

Sircar, S., & Parekh, N. (2015). Functional characterization of drought-responsive modules and genes in *Oryza sativa*: A network-based approach. *Frontiers Genetics*, *6*, 256. https://doi.org/10.3389/fgene.2015.00256

Steyn, W. J., Wand, S. J. E., Holcroft, D. M., & Jacobs, G. (2002). Anthocyanins in vegetative tissues: A proposed unified function in photoprotection. *New Phytologist*, *155*, 349–361. https://doi.org/10.1046/j.1469-8137.2002.00482.x

Stone, J. M., Palta, J. P., Bamberg, J. B., Weiss, L. S., & Harbage, J. F. (1993). Inheritance of freezing resistance in tuber-bearing *Solanum* species: Evidence for independent genetic control of nonacclimated freezing tolerance and cold acclimation capacity. *Proceedings of the National Academy of Sciences of the United States of America*, *90*, 7869–7873. https://doi.org/10.1073/pnas.90.16.7869

Tang, G. Y., Wei, L. Q., Liu, Z. J., Bi, Y. P., & Shan, L. (2012). Ectopic expression of peanut acyl carrier protein in tobacco alters fatty acid composition in the leaf and resistance to cold stress. *Biologia Plantarum*, *56*, 493–501. https://doi.org/10.1007/s10535-012-0057-7

Thomas, J., Kim H. R., Rahmatallah Y., Wiggins G., Yang Q., Singh R., Glazko G., & Mukherjee A. (2019). RNA-seq reveals differentially expressed genes in rice (*Oryza sativa*) roots during interactions with plant-growth promoting bacteria, *Azospirillum brasilense*. *PLoS ONE*, *14*, e0217309. https://doi.org/10.1371/journal.pone.0217309

Vara, C., Paytuví-Gallart A., Cuartero Y., Le Dily F., Garcia F., Salvà-Castro J., Gómez-H L., Julià E., Moutinho C., Aiese Cigliano R., Sanseverino W., Fornas O., Pendás A. M., Heyn H., Waters P. D., Marti-Renom M. A., & Ruiz-Herrera A. (2019). Three-dimensional genomic structure and cohesin occupancy correlate with transcriptional activity during spermatogenesis. *Cell and Reports*, *28*, 352–367. https://doi.org/10.1016/j.celrep.2019.06.037

Vogel, J. T., Zarka, D. G., Van Buskirk, H. A., Fowler, S. G. & Thomashow, M. F. (2005). Roles of the *CBF2* and *ZAT12* transcription factors in configuring the low temperature transcriptome of *Arabidopsis*. *Plant Journal*, *41*, 195–211. https://doi.org/10.1111/j.1365-313X.2004.02288.x

Wang, D., Pei K., Fu Y., Sun Z., Li S., Liu H., Tang K., Han B., & Tao Y. (2007). Genome-wide analysis of the auxin response factors (*ARF*) gene family in rice (*Oryza sativa*). *Gene*, *394*, 13–24. https://doi.org/10.1016/j.gene.2007.01.006

Wang, J., Sun, N., Deng, T., Zhang, L., & Zuo, K. (2014). Genome-wide cloning, identification, classification and functional analysis of cotton heat shock transcription factors in cotton (*Gossypium hirsutum*). *BMC Genomics*, *15*, 961. https://doi.org/10.1186/1471-2164-15-961

Xie, W., Huang, J., Liu, Y., Rao, J., Luo, D., & He, M. (2015). Exploring potential new floral organ morphogenesis genes of *Arabidopsis thaliana* using systems biology approach. *Frontiers in Plant Science*, *6*, 829. https://doi.org/10.3389/fpls.2015.00829

Xue, G. P., Sadat, S., Drenth, J., & McIntyre, C. L. (2014). The heat shock factor family from *Triticum aestivum* in response to heat and other major abiotic stresses and their role in regulation of heat shock protein genes. *Journal of Experimental Botany*, *65*, 539–557. https://doi.org/10.1093/jxb/ert399

Yao, X., Xiong, W., Ye, T., & Wu, Y. (2012). Overexpression of the aspartic protease *ASPG1* gene confers drought avoidance in *Arabidopsis*. *Journal of Experimental Botany*, *63*, 2579–2593. https://doi.org/10.1093/jxb/err433

Zhang, J., Jia, H., Li, J., Li, Y., Lu, M., & Hu, J. (2016). Molecular evolution and expression divergence of the *Populus euphratica Hsf* genes provide insight into the stress acclimation of desert poplar. *Scientific Reports*, *6*, 30050. https://doi.org/10.1038/srep30050

Zhang, J., Li Y., Jia H. X., Li J. B., Huang J., Lu M. Z., & Hu J. J. (2015). The heat shock factor gene family in *Salix suchowensis*: A genome-wide survey and expression profiling during development and abiotic stresses. *Frontiers in Plant Science*, *6*, 748. https://doi.org/10.3389/fpls.2015.00748

Zhou, X., Wang, G., Sutoh, K., Zhu, J. K., & Zhang, W. (2008). Identification of cold-inducible microRNAs in plants by transcriptome analysis. *Biochimica et Biophysica Acta*, *1779*, 780–788. https://doi.org/10.1016/j.bbagrm.2008.04.005

Zhu, M., Xie H., Wei X., Dossa K., Yu Y., Hui S., Tang G., Zeng X., Yu Y., Hu P., & Wang J. (2019). WGCNA analysis of salt- responsive core transcriptome identifies novel hub genes in rice. *Genes*, *10*, 719. https://doi.org/10.3390/genes10090719

SUPPORTING INFORMATION

Additional supporting information may be found online in the Supporting Information section at the end of the article.

How to cite this article: Esposito S, Aversano R, Bradeen J, D'Amelia V, Villano C, Carputo D. Coexpression gene network analysis of cold-tolerant *Solanum commersonii* reveals new insights in response to low temperatures. *Crop Science*. 2021;1-13. https://doi.org/10.1002/csc2.20473